

Adaptive Control for Robot Navigation in Human Environments based on Social Force Model

Chen Wang, Yanan Li, Shuzhi Sam Ge, and Tong Heng Lee

Abstract—In this paper, we introduce a novel control scheme based on the social force model for robots navigating in human environments. Social proxemics potential field is constructed based on the theory of proxemics and used to generate social interaction force for design of robot motion control. A combined kinematic/dynamic control is proposed to make the robot follow the target social force model, in the presence of kinematic velocity constraints. Under the proposed framework, given a specific social convention, robot is able to generate and modify its path smoothly without violating the proxemics constraints. The validity of the proposed method is verified through experimental studies using the V-rep platform.

I. INTRODUCTION

Motion planning and control is a field of mobile robotics which has been extensively studied in the past years. There are many works which demonstrate that robots are able to move and operate in challenging human environments [1]. Among these works, safety and reliability are principal factors to be taken into consideration for successful applications. In [2], safety issues of deployment of a social robot in human environments is studied in detail with respect to various relevant aspects. In [3], humans are modeled as moving obstacles, while [4] proposes a robot navigation method which achieves collision-free robot motion in the presence of moving obstacles. Similarly, there are other works where obstacle avoidance algorithms are developed and dynamic obstacles (humans) are handled in a reactive manner [5], [6]. In [7], a trajectory planning algorithm for a robot operating in dynamic human environments is proposed where a minimal cost trajectory is obtained based on a defined potential field.

While all of these existing methods may be adopted for safe and effective obstacle avoidance of mobile robots, very few of them explicitly take social conventions and rules into account [8]. In general, a robot's ability to adapt its role and behaviors according to social rules and expectation may be a determinant to the success of many applications [9]. In this sense, the generated trajectories are often suboptimal with respect to expectations of humans due to awkward and unexpected evasive movements [10]. Even if a robust obstacle avoidance behavior of the robot can be guaranteed, if the robot fails to signaling social cues which allow humans to feel safe, the comfort of the latter will be greatly affected.

Chen Wang, Shuzhi Sam Ge (corresponding author) and Tong Heng Lee are with the Social Robotics Lab, Interactive & Digital Media Institute (IDMI) and the Department of Electrical & Computer Engineering, National University of Singapore, Singapore 117576 {wang_chen09, samage, eleleeth}@nus.edu.sg

Y. Li is with the Department of Bioengineering, Imperial College London, London SW7 2AZ, UK yli4@imperial.ac.uk

In human-to-robot interactions, a contributing factor to human acceptance of other coexistent agents is how well the robots obey comfortable human-robot spatial relationships [11]. It suggests that humans might perceive a robot as annoying or threatening if it does not show an appropriate distancing behavior [12]. In addition, in [13], it is found that the speed constraints of the mobile robot should also be addressed when investigating the proxemics behavior. It has been shown that humans tend to accepting a robot moving at a slower speed compared to a human's walking speed [11].

Considering the social norm and proxemics constraints, in this paper, we use the social force model introduced in [14] to describe the interactions between robot and human. The social force model is a computational model which describes the interactions between humans by using the concept of social fields or forces. When a target social force model is obtained, the following is to make the robot follow the target social force model. There is much research effort in making a robot track a desired trajectory, including: 1) kinematic control [15], which relies on the assumption that the desired velocities can be quickly established and completely ignores the robot dynamics and the influence of imperfect velocity tracking; 2) a full dynamic model-based control [16], which relies on the assumption that the robot dynamic model is completely known and ignores the uncertainties in the mass, friction and inertia of the robot; and 3) nonlinear adaptive control, which considers the fact that the robot dynamics are nonlinear and include system parameters which are usually uncertain or even unknown. Compared to pure kinematic control and dynamic model-based control, in this paper, we develop a combined adaptive kinematic/dynamic control to handle the dynamic model uncertainties while incorporating the kinematic velocity constraints.

Based on the above discussions, a framework of robot motion control is proposed based on social force model and proxemics theory. A combined adaptive kinematic/dynamic control which considers the control velocity constraints is proposed such that the robot dynamics will be governed by a target social force model. Under the framework, using Lyapunov theory, we show that the mobile robot is able to track the social force model which can be further used to modulate the proxemics spatial relationship between the robot and human.

II. SYSTEM DESCRIPTION

In this paper, we investigate a typical scenario where a wheeled mobile robot navigates in a human environment as shown in Fig. 1. The mobile robot has two driving wheels

mounted along the same axis and a front free wheel. The position of the robot is defined by the vector $p = [x \ y \ \theta]^T$, where x and y are the coordinates of the center of mass of the robot, and θ is the orientation of the robot.

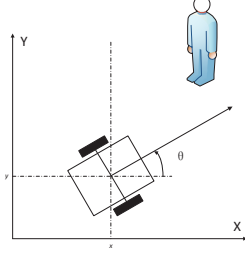


Fig. 1. A nonholonomic mobile robot navigating in human environments

The kinematic model of the mobile robot in terms of its linear velocity v and angular velocity ω is

$$\dot{x} = v \cos(\theta), \quad \dot{y} = v \sin(\theta), \quad \dot{\theta} = \omega \quad (1)$$

which can be further represented as

$$\dot{p} = H(p)z \quad (2)$$

where $z = [v \ \omega]^T$ represents the internal state and $H(p) = [\cos(\theta) \ 0; \sin(\theta) \ 0; 0 \ 1]$. Differentiating \dot{p} results in

$$\ddot{p} = H(p)\dot{z} + \dot{H}(p)z \quad (3)$$

The mobile robot's dynamics and nonholonomic constraint are described by

$$M(p)\ddot{p} + C(p, \dot{p})\dot{p} + G(p) + F(\dot{p}) = B(p)u(t) + J^T(p)\lambda \quad (4)$$

$$J(p)\dot{p} = 0 \quad (5)$$

where $M(p) \in \mathbb{R}^{3 \times 3}$ is a symmetric bounded positive definite inertia matrix, $C(p, \dot{p}) \in \mathbb{R}^3$ denotes the centripetal and Coriolis force, $G(p) \in \mathbb{R}^3$ is the gravitational force, $B(p) \in \mathbb{R}^{3 \times 2}$ is the known input transformation matrix, $F(\dot{p}) \in \mathbb{R}^3$ denotes the generalized friction, $u(t)$ is the system input, $J(p) \in \mathbb{R}^{1 \times 3}$ is the kinematic constraint matrix and λ is the Lagrangian multiplier corresponding to the nonholonomic constraint.

Property 1: [17] There exist some finite positive constants $\psi_j > 0, j = 1, \dots, 4$ such that $\forall p \in \mathbb{R}^3, \forall \dot{p} \in \mathbb{R}^3, \|M(p)\| \leq \psi_1, \|C(p, \dot{p})\| \leq \psi_2 + \psi_3 \|\dot{p}\|$ and $\|G(p)\| + \|F(\dot{p})\| \leq \psi_4$.

For the mobile robot described in Fig. 1, we have the nonholonomic constraint matrix as: $J(p) = [\sin(\theta) \ -\cos(\theta) \ 0]$. From the nonholonomic kinematic constraint, we can easily derive two equations $J(p)\dot{p} = 0$ and $J(p)H(p) = 0$. Substituting the expression for \dot{p} and \ddot{p} into (4) and premultiplying by $H^T(p)$, we have

$$M_1(p)\dot{z} + C_1(p, H(p)z)z + G_1(p) + F_1(p, \dot{p}) = \tau \quad (6)$$

where $M_1(p) = H^T(p)M(p)H(p)$ is a symmetric positive definite inertia matrix, $C_1(p, \dot{p}) = H^T(p)(M(p)\dot{H}(p) + C(p, \dot{p})H(p))$ is the centripetal and Coriolis matrix, $G_1(p) = H^T(p)G(p)$ is the gravity vector, $F_1(p, \dot{p}) = H^T(p)F(\dot{p})$ is the friction, $\tau = B_1(p)u(t)$ is the new system input and

$B_1(p) = H^T(p)B(p)$. In order to fully actuate the nonholonomic system, we assume that the matrix product $H^T(p)B(p)$ is of full rank.

The system (6) describes the original nonholonomic system (5) with a new set of coordinate and the following properties of original system (5) still hold for the new system (6) [18].

Property 2: The generalized inertia matrix $M_1(p)$ is symmetric and positive definite.

Property 3: The matrix $\dot{M}_1(p) - 2C_1(p, \dot{p})$ is skew symmetric.

III. PRELIMINARIES AND DEFINITIONS

A. Social Proxemics and Social Force Model

The term “proxemics” was first proposed in [19] to describe the management of spatial distancing between humans where individuals maintain distances from others. According to [20], the social spaces around a human can be classified into four specific zones where distances from the human body are listed below: 1) public zone: $3.6 \text{ m} \leq l_4$; 2) social zone: $1.2 \text{ m} \leq l_3 < 3.6 \text{ m}$; 3) personal zone: $0.45 \text{ m} \leq l_2 < 1.2 \text{ m}$; and 4) $0 \text{ m} \leq l_1 < 0.45 \text{ m}$.

In a social force model, a robot with mass of m changes its velocity $\dot{\xi}$ as follows

$$m\ddot{\xi} = f_a = f_d + f_i \quad (7)$$

where f_a is the actual force. It can be decomposed into two main parts: robot's desired force f_d and interaction force f_i . Due to the nonholonomic constraint of the mobile robot, θ in p can be uniquely determined given a continuous smooth trajectory, so $\xi = [x \ y]^T$ is a reduced coordinate of p .

Suppose a robot has a desired velocity $\dot{\xi}_d$ where ξ_d is the desired trajectory, the robot's desired force can be described as

$$f_d = \frac{1}{\delta}(\dot{\xi}_d - \dot{\xi}) \quad (8)$$

where δ is the relaxation parameter. Then, the social force model becomes

$$f_i = m\ddot{\xi} + \frac{1}{\delta}(\dot{\xi} - \dot{\xi}_d) \quad (9)$$

B. Social Proxemics Potential Field

In the following, two types of social proxemics potential fields are designed to generate the interaction force f_i . In the first one, the potential field is used to keep the robot out of a certain social zone as shown in Fig. 2(a). The constructed potential field function in this case is designed as

$$U_{sp} = \frac{\alpha}{(\xi - \xi_p)^T Q (\xi - \xi_p) - (R_z^r)^2} \quad (10)$$

where ξ_p is the center of all social zones which is also the human's position, R_z^r is the radius of the circle of the social zone to be kept out of, and Q is a positive definite symmetric matrix which defines the circle shape. In the second one, the potential field is designed for the robot to enter a certain zone while being kept out of another inner zone as shown

in Fig. 2(b). The constructed potential field function for the second case is designed as

$$U_{sp} = \frac{\alpha((\xi - \xi_p)^T Q(\xi - \xi_p) - (R_z^r)^2)}{(\xi - \xi_p)^T Q(\xi - \xi_p) - (R_z^r)^2} \quad (11)$$

where R_z^a is the radius of social zone to be entered.

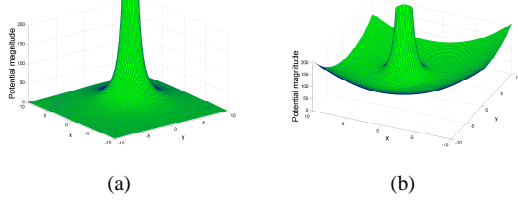


Fig. 2. Social Proxemics Potential Fields

After modeling of the social proxemics potential field, the interaction force f_i can be generated by taking partial derivative of U_{sp} over x and y .

IV. COMBINED ADAPTIVE KINEMATIC/DYNAMIC CONTROL

A. Control Framework

After modeling of the interaction force, the next step is to make the robot dynamics be governed by the social force model in Eq. (9) while considering the velocity constraints. The control objective is to design a control input to make the unknown robot dynamics behave like the desired social force model

$$f_i = m\ddot{\xi}_r + \frac{1}{\delta}(\dot{\xi}_r - \dot{\xi}_d) \quad (12)$$

where $\xi_r = [x_r \ y_r]^T$ is the virtual reference trajectory. In the following sections, combined adaptive kinematic/dynamic control with control velocity constraints will be developed to make $\xi \rightarrow \xi_r$ as $t \rightarrow \infty$, such that the robot dynamics will be governed by the social force model described in Eq. (12).

The proposed control framework is shown in Fig. 3, which can be divided into two parts. In the first part, a social force model is used to modulate the human-aware motion while considering the social proxemics rules. Social proxemics potential field is used to generate the social force used in the social force model. In the second part, a combined adaptive kinematic/dynamic control is adopted for the model matching.

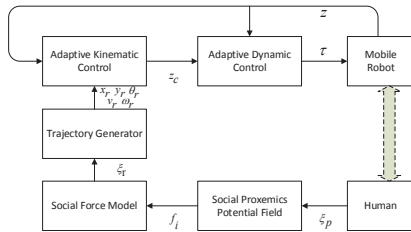


Fig. 3. Control framework

B. Adaptive Kinematic Control with Control Velocity Constraints

System (1) is called the steering system of the robot. To deal with the trajectory tracking problem, similarly to [15], [21], a nonstationary reference pose model that is kinematically identical to the real robot model is employed. The reference trajectory ξ_r can be obtained based on Eq. (12). Using the nonholonomic constraint, the following reference pose model can be obtained:

$$\dot{x}_r = v_r \cos \theta_r, \quad \dot{y}_r = v_r \sin \theta_r, \quad \dot{\theta}_r = \omega_r \quad (13)$$

which can be further represented as

$$\dot{p}_r = H(p_r)z_r \quad (14)$$

where $p_r = [x_r \ y_r \ \theta_r]^T$, $z_r = [v_r \ \omega_r]^T$ and $H(p_r) = [\cos(\theta_r) \ 0; \sin(\theta_r) \ 0; 0 \ 1]$. For trajectory tracking, the error dynamics are written independent of the coordinate frame by Kanayama transformation [15] as

$$\begin{bmatrix} \dot{e}_x \\ \dot{e}_y \\ \dot{e}_\theta \end{bmatrix} = \begin{bmatrix} \cos \theta & \sin \theta & 0 \\ -\sin \theta & \cos \theta & 0 \\ 0 & 0 & 1 \end{bmatrix} (p_r - p) \quad (15)$$

By differentiating Eq. (15), we have

$$\begin{bmatrix} \dot{e}_x \\ \dot{e}_y \\ \dot{e}_\theta \end{bmatrix} = \begin{bmatrix} v_r \cos e_\theta \\ v_r \sin e_\theta \\ \omega_r \end{bmatrix} + \begin{bmatrix} -1 & e_y \\ 0 & -e_x \\ 0 & -1 \end{bmatrix} z \quad (16)$$

which contains the actual velocity z and can be further rewritten as

$$\dot{e} = F_e + G_e z \quad (17)$$

where $e = [e_x; e_y; e_\theta]$, $F_e = [v_r \cos e_\theta; v_r \sin e_\theta; \omega_r]$ and $G_e = [-1 \ e_y; 0 \ -e_x; 0 \ 1]$

To address the issue of imperfect velocity tracking, in this paper, a control velocity $z_c = [v_c \ \omega_c]^T$ is introduced which is subject to the constraints: $-k_j \leq z_{c,j} \leq k_j$, where $j = 1, 2$ and k_j is the known limit of the velocity. An inner-loop controller will be designed to make the actual velocity z converge to z_c with a bounded tracking error $z - z_c$. This will be elaborated in the next subsection.

Considering the presence of control velocity constraints, the following soft saturation is used

$$z_{c,j} = \frac{2k_j}{\pi} \arctan(z_{0,j}) \quad (18)$$

To analyze the velocity constraints during the control design, the following auxiliary system is designed:

$$\dot{\eta} = \begin{cases} -L_1 \eta - (\eta^T)^\dagger |e^T G_e \Delta z|, & \|\eta\| \geq \chi \\ 0, & \|\eta\| < \chi \end{cases} \quad (19)$$

where \dagger denotes the pseudo inverse, $\Delta z = z_c - z_0$, $L_1 = L_1^T > 0$, χ is a small positive parameter to be designed and $\eta \in \mathbb{R}^3$ is the state of the auxiliary system.

Considering a Lyapunov function candidate

$$V_1 = \frac{1}{2} e^T e + \frac{1}{2} \eta^T \eta \quad (20)$$

we have

$$\begin{aligned}\dot{V}_1 &= e^T \dot{e} + \eta^T \dot{\eta} \\ &= -\eta^T L_1 \eta - |e^T G_e \Delta z| + e^T (G_e(z_0 + \Delta z \\ &\quad + z - z_c) + F_e) \\ &\leq -\eta^T L_1 \eta + e^T (G_e(z_0 + z - z_c) + F_e)\end{aligned}\quad (21)$$

Thus, the nominal control input z_0 can be designed such that

$$G_e(z_0 + z - z_c) + F_e = -L_2 e - L_3 \eta \quad (22)$$

where $L_2 = L_2^T > 0$ and $L_3 = L_3^T > 0$ so that

$$\begin{aligned}\dot{V}_1 &\leq -\eta^T L_1 \eta + e^T (-L_2 e - L_3 \eta) \\ &= -\eta^T L_1 \eta - e^T L_2 e - e^T L_3 \eta\end{aligned}\quad (23)$$

Theorem 1: Considering the steering system (1) and the virtual reference system (13), with the auxiliary analysis system (19), control law (22) and proper control parameters L_2 and L_3 , the signal e , η are bounded. In addition, the tracking error e will gradually converge to zero.

Proof: See Appendix VI-A. ■

C. Adaptive Dynamic Control

Using the kinematic control in Sec. IV-B, the control velocity z_c which makes the robot track a desired trajectory can be determined. In the following, an adaptive dynamic control will be proposed such that $z \rightarrow z_c$ as $t \rightarrow \infty$.

Denote the error variable $e_z = z - z_c$, the following Lyapunov function candidate is selected:

$$V_2 = V_{e_z} + V_{\tilde{\psi}}, \quad V_{e_z} = \frac{1}{2} e_z^T M_1 e_z, \quad V_{\tilde{\psi}} = \sum_{j=1}^4 \frac{1}{2b_j} \tilde{\psi}_j^2 \quad (24)$$

where $j = 1, \dots, 4$, $\tilde{\psi}_j = \hat{\psi}_j - \psi_j$, $\hat{\psi}_j$ is the estimate of ψ_j in Property 3 and b_j is a positive constant.

The time-derivative of V_{e_z} is given by

$$\begin{aligned}\dot{V}_{e_z} &= e_z^T \left(\frac{1}{2} \dot{M}_1 e_z + M_1 \dot{e}_z \right) \\ &= e_z^T (\tau - M_1 \dot{z}_c - C_1 z_c - G_1 - F_1)\end{aligned}\quad (25)$$

Considering the definition of ψ_i in Property 1, we have

$$\begin{aligned}& -e_z^T (M_1 \dot{z}_c + C_1 z_c + G_1 + F_1) \\ & \leq \|e_z\| (\|H^T M \dot{H}\| \|\dot{z}_c\| + \|H^T (M \dot{H} + CH)\| \\ & \quad \times \|z_c\| + \|H^T G\| + \|H^T F\|) \\ & \leq \|e_z\| (\psi_1 (\|H^T\| \|H\| \|\dot{z}_c\| + \|H^T\| \|\dot{H}\| \|z_c\|) \\ & \quad + \psi_2 \|H^T\| \|H\| \|z_c\| + \psi_3 \|H^T\| \|\dot{p}\| \|H\| \\ & \quad \times \|z_c\| + \psi_4 \|H^T\|) \\ & = \|e_z\| \sum_{j=1}^4 \psi_j \phi_j\end{aligned}\quad (26)$$

where $\phi_1 = \|H^T\| \|H\| \|\dot{z}_c\| + \|H^T\| \|\dot{H}\| \|z_c\|$, $\phi_2 = \|H^T\| \|H\| \|z_c\|$, $\phi_3 = \|H^T\| \|\dot{p}\| \|H\| \|z_c\|$, $\phi_4 = \|H^T\|$. We propose the adaptive dynamic control as

$$\begin{aligned}\tau &= -K e_z - \sum_{j=1}^4 \frac{\hat{\psi}_j \phi_j^2}{\phi_j \|e_z\| + \sigma_j} e_z \\ \dot{\hat{\psi}}_j &= -a_j \hat{\psi}_j + \frac{b_j \phi_j^2 \|e_z\|}{\phi_j \|e_z\| + \sigma_j}\end{aligned}\quad (27)$$

where $K = K^T > 0$, a_j and σ_j are time-varying positive functions which satisfy $\lim_{t \rightarrow \infty} \sigma_j = 0$ and $\lim_{t \rightarrow \infty} a_j = 0$, respectively.

Theorem 2: Considering the mobile robot dynamics (6), control and parameter adaptation law (27), the velocity track error e_z asymptotically converges to zero, i.e., $\lim_{t \rightarrow \infty} e_z = 0$ with all the signals in the closed-loop bounded.

Proof: See Appendix VI-B. ■

V. EXPERIMENTAL STUDIES

In this section, we verify the validity of the proposed adaptive control through experimental studies. A lumibot with two wheels moves around a human and the human may be static or also walk around [22], as shown in Fig. 4. This experiment is implemented with the Virtual Robot Experimentation Platform (V-Rep) which is an open-source robot simulation platform [23].

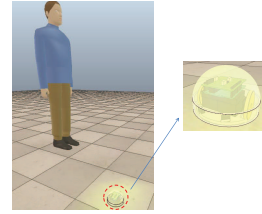


Fig. 4. Experimental scenario. A lumibot with two wheels moves around a human and the human may be static or also walk around.

In the first part of the studies, the effectiveness of the combined adaptive kinematic/dynamic control is verified. The robot is supposed to track a predefined desired trajectory. The kinematic control velocity constraints are selected as $\|\omega\| \leq 0.3$ rad/s and $\|v\| \leq 0.35$ m/s. The reference trajectory is given as: $x_r(t) = 0.1t$, $y_r(t) = \sin(x_r(t))$. The robot's initial posture is set as $[-0.5 \ 0.5 \ \frac{\pi}{3}]^T$. The control parameters are designed as $L_1 = 10I_{3 \times 3}$, $L_2 = 20I_{3 \times 3}$, $L_3 = 20I_{3 \times 3}$, $\chi = 0.02$, $K = 15I_{2 \times 2}$, $b_j = 0.01$ and $a_j = \sigma_j = e^{-0.01t}$ where $j = 1, \dots, 4$ and $I_{n \times n}$ is the n -by- n identity matrix.

The experimental results are shown in Figs. 5, 6 and 7. From Figs. 5 and 6, it is found that the actual trajectory under the proposed method can accurately track the desired one and the defined errors are quite small. The velocity constraints applied on the control velocity can be reflected from Fig. 7 which indicates that the control velocity never transgresses the constraints during the whole process.

In the second part, we will investigate the effectiveness of the social force model in human environments. The parameters in the social force model are selected as $M = 0.5$, $\delta = 0.01$ and the parameter in the social proxemics potential field, α , is selected as 0, 0.5, 1 and 2 for comparison. When $\alpha = 0$, it means that the robot will no longer be influenced

by human and thus the robot's actual trajectory will track the desired trajectory.

In case 1, as shown in Fig. 8, the robot is navigating in a human environment where the human is static. It can be observed that although the desired trajectory of the robot invades the personal zone, under the proposed control, the proxemics constraints are not violated. As the social norms are not strict and vary with age, culture, type of relationship and context, they can be reflected by adjusting the parameter α . From Fig. 8, we can find that the robot trajectory deviates more from the desired trajectory if a larger α is selected. In case 2, as shown in Fig. 9, the robot is navigating and engaging in a close social interaction with human. In this case, the robot enters the personal zone while being kept out of the intimate zone. In case 3, the robot is following a human. The desired trajectory of the robot will be the trajectory of the human. In this case, the robot will follow the human to enter the personal zone while not intruding the intimate zone. The experimental results are shown in Fig. 10. From the experimental results, it can be observed that the proposed adaptive control based on social force model can effectively address the problem of human-aware motion control.

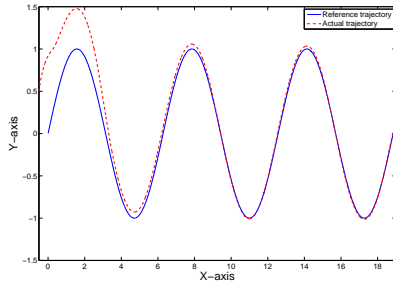


Fig. 5. Desired and actual trajectories

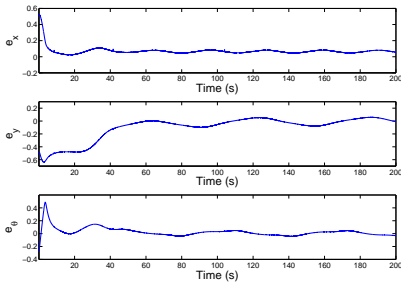


Fig. 6. Tracking error

VI. CONCLUSION

In this paper, we have presented the design of an adaptive control based on social force model for mobile robots operating in human environments. A combined adaptive kinematic/dynamic control has been applied to guarantee that the target social force model is achieved. The validity of the proposed method has been verified by experimental studies.

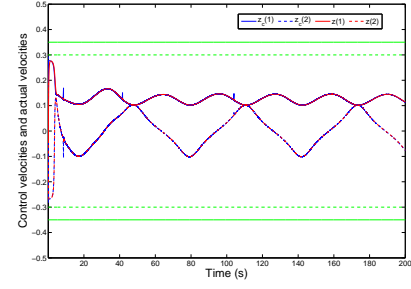


Fig. 7. Control velocity and actual velocity. Constraints on v are denoted using green solid line and constraints on ω are represented using green dashed line.

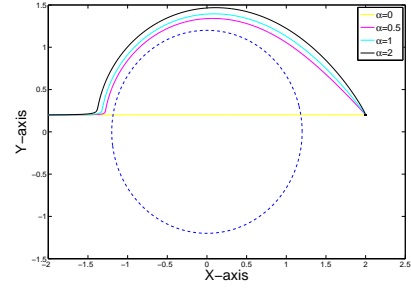


Fig. 8. Case 1: Robot being kept out of a social zone. The blue dashed line describes the boundary of the personal zone.

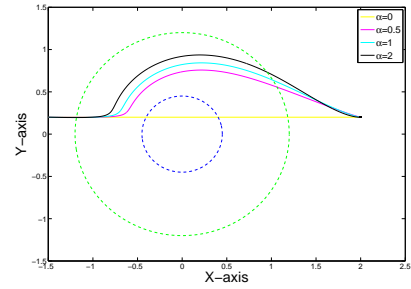


Fig. 9. Case 2: Robot entering the personal zone while being kept out of the intimate zone. The green dashed line describes the boundary of the personal zone. The blue dashed line describes the boundary of the intimate zone.

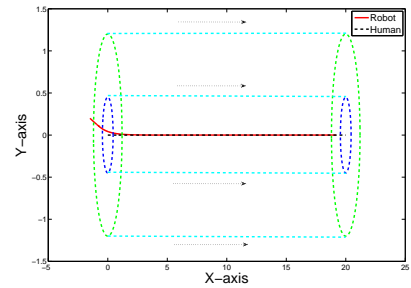


Fig. 10. Case 3: Robot following a human while being kept out of the intimate zone. The green dashed line describes the boundary of the personal zone. The blue dashed line describes the boundary of the intimate zone. The black dotted array and cyan dashed lines describe the movement of the human and zone boundaries.

A. Proof of Theorem 1

With $\sigma > 0$, it is clear that $-e^T L_3 \eta \leq 0.5\sigma e^T e + 0.5\sigma^{-1}\eta^T L_3^T L_3$. Invoking it into Eq. (23), we have

$$\begin{aligned} \dot{V}_1 &= -\eta^T (L_1 - 0.5\sigma^{-1} L_3^T L_3) \eta \\ &\quad - e^T (L_2 - 0.5\sigma) e \leq -\rho V_1 \end{aligned} \quad (28)$$

where $\rho = \min(2\lambda_{\min}(L_1 - 0.5\sigma^{-1} L_3^T L_3), 2\lambda_{\min}(L_2 - 0.5\sigma))$. To ensure that ρ is positive, the parameters L_1, L_2, L_3 and σ can be selected to satisfy the following conditions

$$\lambda_{\min}(L_1 - \sigma^{-1} L_3^T L_3) > 0, \lambda_{\min}(L_2 - \sigma) > 0 \quad (29)$$

Ineq. (28) indicates that $V_1(t) \leq V_1(0)e^{-\rho t}$, then it is easy to derive that $V_1(t)$ and all the close-loop signals are bounded and $e \rightarrow 0$ as $t \rightarrow \infty$ [24].

B. Proof of Theorem 2

By differentiating V_2 in Eq. (24), we obtain

$$\begin{aligned} \dot{V}_2 &= \dot{V}_{e_z} + \dot{V}_{\tilde{\psi}} \\ &= e_z^T (-K e_z - \sum_{j=1}^4 \frac{\psi_j \phi_j^2}{\phi_j \|e_z\| + \sigma_j} e_z - M_1 \dot{z}_c \\ &\quad - C_1 \dot{z}_c - G_1 - F_1) + \sum_{j=1}^4 \frac{a_j}{b_j} \tilde{\psi}_j \dot{\psi}_j \end{aligned} \quad (30)$$

Substituting the control and updating law (27) into Eqs. (24) and (25), and using the inequality in Eq. (26), we have

$$\begin{aligned} \dot{V}_2 &\leq -e_z^T K e_z + \sum_{j=1}^4 \sigma_j \psi_j + \sum_{j=1}^4 \frac{a_j}{b_j} \tilde{\psi}_j \dot{\psi}_j \\ &\leq -e_z^T K e_z + \varepsilon \end{aligned} \quad (31)$$

where $\varepsilon = \sum_{j=1}^4 \sigma_j \psi_j + \frac{1}{4} \sum_{j=1}^4 \frac{a_j}{b_j} \psi_j^2$. Because $\lim_{t \rightarrow \infty} \sigma_j = 0$ and $\lim_{t \rightarrow \infty} a_j = 0$, we have $\lim_{t \rightarrow \infty} \varepsilon = 0$. Integrating both sides of the above inequality, we can derive

$$\int_0^t e_z^T K e_z dt \leq V_2(0) + \int_0^t \delta(t) dt \quad (32)$$

Thus, we have

$$V_2(t) \leq V_2(0) - \int_0^t e_z^T K e_z dt + \int_0^t \delta(t) dt \quad (33)$$

As $\lim_{t \rightarrow \infty} \varepsilon = 0$ and $V_2(0)$ are bounded, $V_2(t)$ and $\int_0^t e_z^T K e_z dt$ are bounded, which results in $e_z \in L_2^n$. According to Barbalet's Lemma [25], $e_z \in L_2^n$ and $\dot{e}_z \in L_\infty^n$ lead to $e_z \rightarrow 0$.

REFERENCES

- [1] W. Burgard, A. B. Cremers, D. Fox, D. Hähnel, G. Lakemeyer, D. Schulz, W. Steiner, and S. Thrun, "Experiences with an interactive museum tour-guide robot," *Artificial intelligence*, vol. 114, no. 1, pp. 3–55, 1999.
- [2] R. Alami, A. Albu-Schaeffer, A. Bicchi, R. Bischoff, R. Chatila, A. De Luca, A. De Santis, G. Giralt, J. Guiochet, G. Hirzinger, et al., "Safe and dependable physical human-robot interaction in anthropic domains: State of the art and challenges," in *2006 IEEE/RSJ International Conference on Intelligent Robots and Systems (IROS)*, pp. 1–16, 2006.
- [3] E. Trulls, A. Corominas Murtra, J. Pérez-Ibarz, G. Ferrer, D. Vasquez, J. M. Mirats-Tur, and A. Sanfeliu, "Autonomous navigation for mobile service robots in urban pedestrian environments," *Journal of Field Robotics*, vol. 28, no. 3, pp. 329–354, 2011.
- [4] P. Trautman, "Probabilistic tools for human-robot cooperation," in *Human Agent Robot Teamwork Workshop HRI*, 2012.
- [5] B. Kluge and E. Prassler, "Recursive agent modeling with probabilistic velocity obstacles for mobile robot navigation among humans," in *Autonomous Navigation in Dynamic Environments*, pp. 121–134, Springer, 2007.
- [6] A. S. Matveev, C. Wang, and A. V. Savkin, "Real-time navigation of mobile robots in problems of border patrolling and avoiding collisions with moving and deforming obstacles," *Robotics and Autonomous systems*, vol. 60, no. 6, pp. 769–788, 2012.
- [7] M. Svenstrup, T. Bak, and H. J. Andersen, "Trajectory planning for robots in dynamic human environments," in *2010 IEEE/RSJ International Conference on Intelligent Robots and Systems (IROS)*, pp. 4293–4298, 2010.
- [8] A. K. Pandey and R. Alami, "A framework towards a socially aware mobile robot motion in human-centered dynamic environment," in *2010 IEEE/RSJ International Conference on Intelligent Robots and Systems (IROS)*, pp. 5855–5860, 2010.
- [9] Y. Li, K. Tee, S. S. Ge, and H. Li, "Building companionship through human-robot collaboration," in *Social Robotics* (G. Herrmann, M. Pearson, A. Lenz, P. Bremner, A. Spiers, and U. Leonards, eds.), vol. 8239 of *Lecture Notes in Computer Science*, pp. 1–7, Springer International Publishing, 2013.
- [10] M. Kuderer, H. Kretzschmar, C. Sprunk, and W. Burgard, "Feature-based prediction of trajectories for socially compliant navigation," in *Robotics: science and systems*, 2012.
- [11] L. Takayama and C. Pantofaru, "Influences on proxemic behaviors in human-robot interaction," in *2009 IEEE/RSJ International Conference on Intelligent Robots and Systems (IROS)*, pp. 5495–5502, 2009.
- [12] B. Mutlu and J. Forlizzi, "Robots in organizations: the role of workflow, social, and environmental factors in human-robot interaction," in *2008 3rd ACM/IEEE International Conference on Human-Robot Interaction (HRI)*, pp. 287–294, 2008.
- [13] J. T. Butler and A. Agah, "Psychological effects of behavior patterns of a mobile personal robot," *Autonomous Robots*, vol. 10, no. 2, pp. 185–202, 2001.
- [14] D. Helbing and P. Molnar, "Social force model for pedestrian dynamics," *Physical review E*, vol. 51, no. 5, p. 4282, 1995.
- [15] Y. Kanayama, Y. Kimura, F. Miyazaki, and T. Noguchi, "A stable tracking control method for an autonomous mobile robot," in *1990 IEEE International Conference on Robotics and Automation (ICRA)*, pp. 384–389, IEEE, 1990.
- [16] M. L. Corradini and G. Orlando, "Robust tracking control of mobile robots in the presence of uncertainties in the dynamical model," *Journal of Robotic Systems*, vol. 18, no. 6, pp. 317–323, 2001.
- [17] Y. Li and S. S. Ge, "Human-robot collaboration based on motion intention estimation," *IEEE/ASME Transactions on Mechatronics*, vol. 19, no. 3, pp. 1007–1014, 2014.
- [18] R. Fierro and F. L. Lewis, "Control of a nonholonomic mobile robot: backstepping kinematics into dynamics," in *1995 IEEE Conference on Decision and Control (CDC)*, vol. 4, pp. 3805–3810, IEEE, 1995.
- [19] E. T. Hall, "A system for the notation of proxemic behavior1," *American anthropologist*, vol. 65, no. 5, pp. 1003–1026, 1963.
- [20] T. Edward, "Hidden dimension: Man's use of space in public and private," in *The Boley Hear Ltd, London*, 1966.
- [21] C. C. De Wit, H. Khenouf, C. Samson, and O. J. Sordalen, "Nonlinear control design for mobile robots," *Recent trends in mobile robots*, vol. 11, pp. 121–156, 1993.
- [22] M. L. Kronemann and V. V. Hafner, "Lumibots: making emergence graspable in a swarm of robots," in *Proceedings of the 8th ACM Conference on Designing Interactive Systems*, pp. 408–411, 2010.
- [23] S. Dura-Bernal, G. L. Chadderdon, S. A. Neymotin, J. T. Francis, and W. W. Lytton, "Towards a real-time interface between a biomimetic model of sensorimotor cortex and a robotic arm," *Pattern Recognition Letters*, vol. 36, pp. 204–212, 2014.
- [24] S. S. Ge, C. C. Hang, T. H. Lee, and T. Zhang, *Stable Adaptive Neural Network Control*. Norwell, USA: Kluwer Academic, 2001.
- [25] V. M. Popov and R. Georgescu, *Hyperstability of control systems*. Springer-Verlag New York, Inc., 1973.